

## Observations of residual bulk-fluid motion and low-mode areal-density asymmetries near peak convergence in NIF implosions through spectral measurements of DD and DT neutrons

J.A. Frenje<sup>1</sup>, B. Appelbe<sup>5</sup>, R.M. Bionta<sup>2</sup>, E.J. Bond<sup>2</sup>, D.K. Bradley<sup>2</sup>, J.A. Caggiano<sup>2</sup>, D.A. Callahan<sup>2</sup>, D.T. Casey<sup>2</sup>, C.J. Cerjan<sup>2</sup>, J. Chittenden<sup>5</sup>, T. Döppner<sup>2</sup>, M.J. Eckart<sup>2</sup>, M.J. Edwards<sup>2</sup>, V.Yu. Glebov<sup>3</sup>, G.P. Grim<sup>2</sup>, E.P. Hartouni<sup>2</sup>, R. Hatarik<sup>2</sup>, D.E. Hinkel<sup>2</sup>, O.A. Hurricane<sup>2</sup>, W.W. Hsing<sup>2</sup>, M. Gatu Johnson<sup>1</sup>, J.D. Kilkenny<sup>4</sup>, J.P. Knauer<sup>3</sup>, A. Kritcher<sup>2</sup>, D.H. Munro<sup>2</sup>, T. Murphy<sup>6</sup>, O.L. Landen<sup>2</sup>, S. LePape<sup>2</sup>, T. Ma<sup>2</sup>, N. Meezan<sup>2</sup>, P. Patel<sup>2</sup>, R.D. Petrasso<sup>1</sup>, T.C. Sangster<sup>3</sup>, D.B. Sayre<sup>2</sup>, B.K. Spears<sup>2</sup>, P.T. Springer<sup>2</sup> and C.B. Yeaman<sup>2</sup>

<sup>1</sup>Massachusetts Institute of Technology, Cambridge, MA 02139, USA

<sup>2</sup>Lawrence Livermore National Laboratory, Livermore, CA 94550, USA

<sup>3</sup>Laboratory for Laser Energetics, University of Rochester, Rochester, NY 14623, USA

<sup>4</sup>General Atomics, San Diego, CA 92186, USA

<sup>5</sup>Imperial College London, South Kensington SW7 2AZ, United Kingdom

<sup>6</sup>Los Alamos National Laboratory, Los Alamos, New Mexico 87545, USA

*E-mail contact of main author: jfrenje@psfc.mit.edu*

**Abstract.** In recent high-foot-implosion experiments at the National Ignition Facility (NIF), directional measurements of the Inertial Confinement Fusion (ICF) neutron spectrum illustrate the existence of substantial bulk-fluid motion and low-mode areal-density ( $\rho R$ ) asymmetries near peak convergence, which significantly degrade the implosion performance. Measured energy shifts of the primary neutron spectrum, beyond ion-temperature-induced shifts, indicate bulk-fluid motions up to about 50 km/s. The measured width of the primary neutron spectrum, which is broadened by the variance of the bulk-fluid motion and thermal ion temperature in the burning region, is also indicative of substantial bulk-fluid motion. The reason for this is that the measured apparent DT ion temperature (DT-“ $T_i$ ”) is consistently higher than the DD-“ $T_i$ ”, a discrepancy that increases with increasing implosion velocity, which cannot be explained by profiles and reactivity differences. Three-dimensional (3D) asymmetries and bulk-fluid motion must be invoked in the modelling of the measured apparent ion temperatures. Directional yield measurements of scattered neutrons and un-scattered neutrons also indicate  $\rho R$  asymmetries up to about  $\pm 500$  mg/cm<sup>2</sup> in the layer of cold and dense fuel surrounding the hot spot. The hypothesis is that these observations are mainly driven by radiation drive asymmetries and instabilities seeded by the fill tube and thin tent holding the capsule in the Hohlraum, which are currently being addressed by new engineering solutions, more refined implosion modeling and implementation of new diagnostics.

### 1. Introduction

Hot-spot ignition planned at the National Ignition Facility (NIF) [1] requires proper assembly of the DT fuel, as manifested by the evolution of areal-density ( $\rho R$ ) symmetry and hot-spot thermal ion temperature ( $T_i$ ). Ideally, a spherically symmetric layer of cold and dense fuel with a  $\rho R$  exceeding 1 g/cm<sup>2</sup> surrounding a  $\sim 5$  keV lower-density hot spot is obtained at peak convergence [2]. To reach these conditions, the implosion must be one-dimensional (1D) in nature, and efficient conversion of the implosion kinetic energy to hot-spot thermal energy must be obtained. If substantial 3D asymmetries exist in the implosion, the conversion efficiency is degraded and significant fraction of the implosion kinetic energy, in the form of bulk-fluid motion, remains at peak convergence [3-5].

Experimentally, the residual bulk-fluid motion is assessed from directional measurements of the primary ICF neutron spectrum [6-10] using five spectrometers on the NIF (*FIG. 1*). Energy shifts beyond  $T_i$ -induced shifts are indicative of bulk-fluid motion [11]. The width of the primary spectrum is also an indication of  $T_i$  and the variance of the bulk-fluid motion in the burning region. Additionally,  $\rho R$  asymmetries are determined from directional yield measurements of scattered or un-scattered neutrons [12-14].

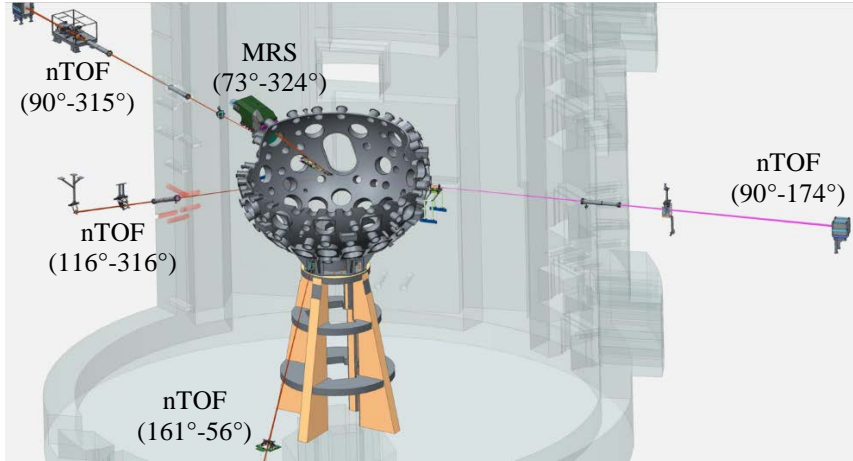


FIG. 1. A cross-cut drawing of the NIF chamber, which illustrates the locations of four neutron-Time-Of-Flight (nTOF) spectrometers [15] and the Magnetic Recoil Spectrometer (MRS) [16-17] for directional measurements of the ICF neutron spectrum, from which yield, apparent  $T_i$  (“ $T_i$ ”),  $\rho R$  asymmetries and bulk-fluid motion are determined.

## 2. Observations

### 2.1 Energy shifts of the primary neutron spectrum due to bulk-fluid motion

From the measured energy shift of the primary neutron spectrum, the bulk-fluid motion has been determined after the  $T_i$ -induced energy shift has been corrected for. While a finite  $T_i$  always increases the mean energy of the primary neutron peak, the bulk-fluid motion will either “red shift” or “blue shift” the spectrum, depending on the velocity vector relative to the diagnostic Line-Of-Sight (LOS). For the DT reaction, the relationship between the bulk-fluid motion ( $V_{CM}$ ) along the diagnostic LOS and the energy shift ( $\Delta E_n$ ) can be approximated by [6]

$$V_{CM} \approx 1.85 \cdot \Delta E_n, \quad (1)$$

where  $V_{CM}$  is given in km/s and  $\Delta E_n$  is given in keV. FIG. 2 illustrates the bulk-fluid motion determined from energy shifts measured by three nTOF detectors shown in FIG. 1. As shown by the data, bulk-fluid motion up to about 50 km/s are observed along the different diagnostic LOS. Although the data might be weakly anti-correlated, it is not clear if the bulk-fluid motion is near isotropic (radial) or non-isotropic in nature. It is also not clear what is causing these perturbations.

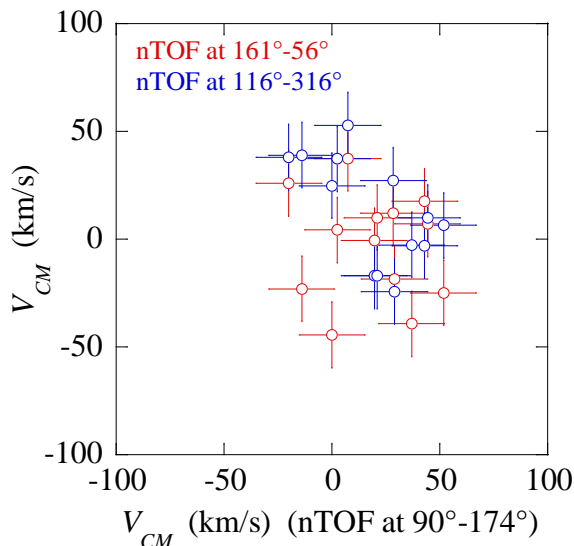


FIG. 2. Bulk-fluid motion measured by the nTOFs positioned at 161°-56° and 116°-56° as function of bulk-fluid motion along nTOF LOS 90°-174°. The measurement uncertainties are 15 km/s. The data set suggests a weak anti-correlation, but further analysis is required before any conclusions can be drawn.

## 2.2 Anomalous hot-spot temperature differences

The apparent DD and DT burn-averaged ion temperature “ $T_i$ ” (DD-“ $T_i$ ” and DT-“ $T_i$ ”) are obtained from measurements of the spectral widths of the DT and DD primary neutron spectra. If bulk-fluid motion is insignificant, these two measurements are expected to only differ by  $\sim 5\%$ , due to profiles and differences in reactivities, since they have different weightings over the temperature distribution of the hot spot. FIG. 3a shows that for implosions where DT-“ $T_i$ ” is  $< 4$  keV, the DD-“ $T_i$ ” and DT-“ $T_i$ ” are self-consistent and described relatively well by 1D modeling, but as the implosion velocity and the DT-“ $T_i$ ” increases above 4 keV the two measurements increasingly diverge. At the highest implosion velocities, a DT-“ $T_i$ ” of about 6 keV and DD-“ $T_i$ ” of about 5 keV, or a differential of  $\Delta T_i = 1$  keV, are measured and compared to an expected  $\Delta T_i$  of about 0.3 keV. In these cases, the measurements are also 0.5-1 keV higher than 2D simulations [3]. To reconcile these observations, bulk-fluid motion needs to be considered in the modeling, as discussed in the next paragraph.

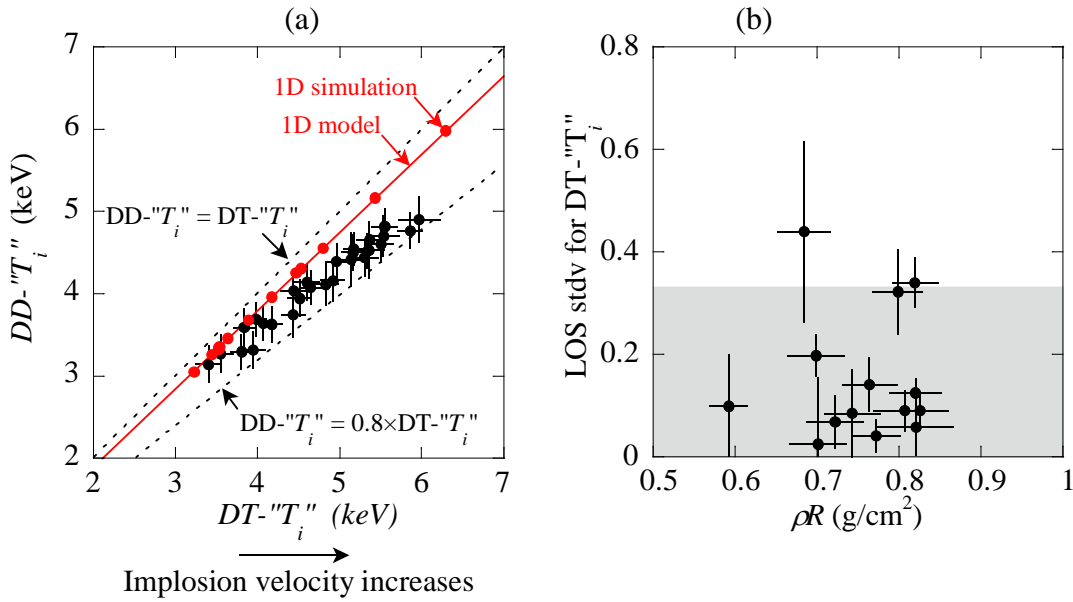


FIG. 3. (a) DD-“ $T_i$ ” versus DT-“ $T_i$ ” (black data points). For comparison, 1D modeling that considers profiles and reactivity differences is shown by the solid red line. 1D simulations are shown by the red data points. The two black dashed lines illustrate DD-“ $T_i$ ” = DT-“ $T_i$ ” and DD-“ $T_i$ ” =  $0.8 \times$  DT-“ $T_i$ ” dependencies, which bracket the data. The data start deviating at higher apparent temperatures (or higher implosions velocities [5]). (b) Observed LOS variation in the observed DT-“ $T_i$ ” as function of measured average  $\rho R$  for a subset of the high-foot implosions. Each data point represents one implosion. The gray region represents an estimate of the systematic uncertainty in the individual measurements.

As extensively discussed in references [6-11], the width of the neutron spectrum for an evolving plasma is affected by both the hot-spot thermal  $T_i$  and residual bulk-fluid motion as described by

$${}^{\prime}T_i = T_i + \frac{m_d + m_x}{k_B} \sigma_v^2, \quad (2)$$

where  $T_i$  is the thermal burn-averaged temperature,  $m_d$  is the mass of the deuteron,  $m_x = m_d$  for DD reactions and  $m_x = m_t$  (triton mass) for DT reactions,  $k_B$  is Boltzmann’s constant and  $\sigma_v^2$  is the variance of the bulk-fluid velocities along the diagnostic LOS. If the variance of the bulk-fluid velocity is the dominating term, then the inferred DD-“ $T_i$ ” will be about 80% of the DT-

“ $T_i$ “, which is close to the observations in the high-velocity and high-“temperature” implosion experiments (*FIG. 3a*). This would suggest that substantial bulk-fluid motion is present in these implosions and that the true thermal  $T_i$  is significantly lower than the measured “ $T_i$ “. However, a much lower thermal  $T_i$  cannot explain the observed neutron yields [11], and other factors such as 3D asymmetries must also be invoked in the modeling. In addition, *FIG. 3b* shows the observed LOS isotropy as a function of measured average  $\rho R$  for a subset of the high-foot implosions. Relatively little variation is observed across the individual measurements of DT-“ $T_i$ “, indicating no strong evidence for large anisotropic flows in the hot-spot (but strong isotropic flows can still be present) [10].

### 2.3 Substantial low-mode $\rho R$ asymmetries

Substantial low-mode  $\rho R$  asymmetries in the layer of cold and dense fuel, surrounding the hot spot, have been determined from both flange nuclear activation detectors (FNADs) [13] and neutron spectrometry [12,14]. The FNADs measure the relative directional yield of unscattered primary neutrons at nineteen locations around the implosion relative to the global average  $Y_n(\text{ave})$ , from which a 3D relative  $\rho R$  map is inferred. An example of a  $\rho R$  map for implosion N150422 is shown in *FIG. 4*, which shows a low-mode  $\rho R$  asymmetry of  $\pm 500$  mg/cm<sup>2</sup>. This observation is also supported by down-scattered neutron measurements using neutron spectrometry located by the black points shown in *FIG. 4*.

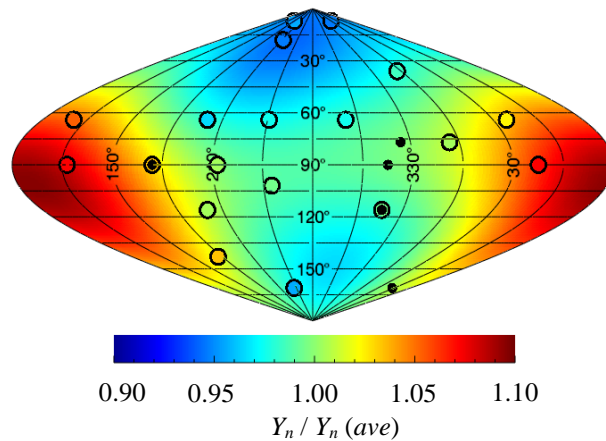


*FIG. 4.*  $Y_n/Y_n(\text{ave})$  ratio for shot N150422 measured with flange nuclear activation detectors (positions indicated by the open circles). Smaller black data points indicate the positions of the nTOFs and the MRS used for down-scattered neutron measurements, from which a  $\rho R$  can be determined. The color map was generated by fitting a low-order spherical harmonics to the data. A  $Y_n/Y_n(\text{ave})$  variation of about  $\pm 10\%$  is observed in this particular case, which roughly corresponds to a  $\rho R$  asymmetry of about  $\pm 500$  mg/cm<sup>2</sup>.

On approximately 50% of the high-foot implosions, the FNADs data are fit with spherical harmonics with modal content up to  $L=2$ , which generally show regions of high  $\rho R$  at the poles (blue areas in the figure). The other 50% of the data show residual RMS deviation from the  $L=2$  fit, implying the existence of  $L$ -modal content  $> 2$ . Models of the hot spot and cold fuel with only simple low-mode shape distortions struggle to predict this excess RMS at modes  $L>2$ . In this context, it should be noted that this interpretation of equivalency between directional unscattered neutrons and  $\rho R$  is only valid for a quasi-spherical hot-spot surrounded by a dense fuel layer. In the case of very distorted hot spots, the variation in FNADs data may be low despite the existence of high  $\rho R$  values at the poles. To address this issue, new diagnostics are being implemented for more accurate diagnosis of the cold and dense fuel

surrounding the hot spot. A new analysis method is also been developed to isolate an image of the cold fuel by using the primary neutron image to compensate for the flux from the hot spot [18]. Preliminary analysis using this method show regions of higher cold fuel mass at the poles, consistent with inferences of the FNADs data.

### 3. Hypotheses for the observations and path forward

A number of hypotheses have been formulated for explaining these observations and identifying the sources for performance degradation relative to expectations and detailed post-shot simulations. The leading hypotheses are:

- Radiation drive asymmetry. The limited accuracy of the physics models for high-gas-fill hohlraums restricts the ability to accurately predict the radiation flux asymmetry on the capsule from initial laser and capsule parameters. Post-shot simulations that are tuned to best match the observables suggest that radiation drive asymmetry is the dominant source of degradation, and that its impact increases significantly with increasing implosion velocity.
- Instabilities seeded by the fill tube and thin tent holding the capsule in the Hohlraum. Focused implosion experiments reveal a relatively small  $\rho R$  perturbation arising from the tens-of-nanometer-thick tent holding the capsule in the hohlraum. There appears to be evidence of "pinching" of the hot spot induced by the tent in x-ray self-imaging of implosion N140819, the thinnest ablator, highest-velocity implosion. A 3D simulation of this implosion predicts significant growth of the tent perturbation and localized thinning of the high-density layer at stagnation, suggesting that the implosion is on the verge of break-up and loss of confinement. In addition, time-resolved x-ray self-emission measurements sometimes show features that might originate from the fill-tube, though the measurements are not conclusive. X-ray measurements suggest that the fill-tube may affect both the hot-spot shape and the  $\rho R$  uniformity in surrounding layer of cold and dense fuel. Recent experiments also show evidence of the fill-tube seeding a much larger perturbation than currently predicted in simulations.

These hypotheses are currently being addressed by implementing new engineering solutions, more refined modeling and implementation of new diagnostics. Some of the diagnostics that are being implemented are:

- A high-accuracy Ross-pair spectrometer for measurements of the x-ray continuum slope from which an emissivity-weighted  $T_e$  can be determined and contrasted to the neutron-averaged apparent  $T_i$  [19].
- 30 additional FNADs, which will enable the relative fuel  $\rho R$  distribution to be resolved up to mode  $L=4$ , compared to the current limit of  $L=2$ .
- Compton radiography to measure shape and  $\rho R$  distribution of the surrounding layer of cold and dense fuel. [20].
- The Magnet Recoil Spectrometer (MRSt) for simultaneous time-resolved measurements of neutron rate, apparent  $T_i$ , residual flow velocities and fuel  $\rho R$  [21].

#### 4. Summary

Directional measurements of the ICF neutron spectrum illustrate the existence of substantial bulk-fluid motion up to about 50 km/s and low-mode  $\rho R$  asymmetries up to about  $\pm 500$  mg/cm<sup>2</sup> near peak convergence, which significantly degrade the implosion performance. The measured DT- $T_i$  is also consistently higher than the DD- $T_i$ , a discrepancy that increases with increasing implosion velocity. Effects due to profiles and reactivity differences cannot explain this discrepancy, and 3D asymmetries and bulk-fluid motion must be invoked in the modelling of these data. The hypothesis is that these observations are mainly driven by radiation drive asymmetries and instabilities seeded by the fill-tube and thin tent holding the capsule in the Hohlraum, which are currently being addressed by new engineering solutions, more refined implosion modeling and implementation of new diagnostics. This material is based on work supported in part by the U.S. Department of Energy under the contract DE-AC52-07NA27344.

#### References

- [1] MILLER, G.H. et al., “The National Ignition Facility: Ushering in a new age for high energy density science”, Nucl. Fusion 44, S228 (2004).
- [2] EDWARDS M.J. et al., “Progress towards ignition on the National Ignition Facility”, Phys. Plasmas 20, 070501 (2013).
- [3] HURRICANE O.A. et al., “Inertially confined fusion plasmas dominated by alpha-particle self-heating”, Nature Phys., page 1, 11 April 2016.
- [4] CLARK D.S. et al., “Three-dimensional simulations of low foot and high foot implosion experiments on the National Ignition Facility”, Phys. Plasmas 23, 056302 (2016).
- [5] KRITCHER A.L. et al., “Integrated modeling of cryogenic layered highfoot experiments at the NIF”, Phys. Plasmas 23, 052709 (2016).
- [6] GATU JOHNSON M., “Measurements of collective fuel velocities in deuterium-tritium exploding pusher and cryogenically layered deuterium-tritium implosions on the NIF”, Phys. Plasmas 20, 042707 (2013).
- [7] APPELBE B. et al., “The production spectrum in fusion plasmas”, 53 (2011) 045002.
- [8] MUPHY T.J. et al., “The effect of turbulent kinetic energy on inferred ion temperature from neutron spectra”, Phys. Plasmas 21, 072701 (2014).
- [9] MUNRO D.H., “Interpreting inertial fusion neutron spectra”, Nucl. Fusion 56 (2016) 036001.
- [10] CHITTENDEN J.P. et al., “Signatures of asymmetry in neutron spectra and images predicted by three-dimensional radiation hydrodynamics simulations of indirect drive implosions”, Phys. Plasmas 23, 052708 (2016).
- [11] GATU JOHNSON M., “Indications of flow near maximum compression in layered DT implosions at the National Ignition Facility”. Phys. Rev. E 94, 021202(R) (2016).
- [12] FRENJE J.A. et al., “Diagnosing implosion performance at the National Ignition Facility (NIF) by means of neutron spectrometry”, Nucl. Fusion 53, 043014 (2013).
- [13] YEAMANS C.B. et al., “Enhanced NIF neutron activation diagnostics”, Rev. Sci. Instrum. 83, 10D315 (2012).
- [14] GATU JOHNSON M., “Neutron spectrometry – An essential tool for diagnosing implosions at the National Ignition Facility”, Rev. Sci. Instrum. 83, 10D308 (2012).

- [15] HATÁRIK R. et al., “Analysis of the neutron time-of-flight spectra from inertial confinement fusion experiments“, J. Applied Phys. 118, 184502 (2015).
- [16] FRENJE J.A. et al., “Probing high areal-density cryogenic deuterium-tritium implosions using downscattered neutron spectra measured by the magnetic recoil spectrometer“, Phys. Plasmas 17, 056311 (2010).
- [17] CASEY D.T. et al., “The magnetic recoil spectrometer for measurements of the absolute neutron spectrum at OMEGA and the NI“, Rev. Sci. Instrum. 84, 043506 (2013).
- [18] CASEY D.T. et al., “Fluence-Compensated Down-scattered Neutron Imaging using the Neutron Imaging System at the National Ignition Facility“, Rev. Sci. Instrum. 87 11E715 (2016).
- [19] JARROTT L.C. et al., “Hotspot electron temperature from x-ray continuum measurements on the NIF“, Rev. Sci. Instrum. 87, 11E534 (2016).
- [20] HALL G.N. et al., “Spatial resolution measurements of the advanced radiographic capability x-ray imaging system at energies relevant to Compton radiography“, Rev. Sci. Instrum. 87, 11E310 (2016).
- [21] FRENJE J.A. et al., “The magnetic recoil spectrometer (MRSt) for time-resolved measurements of the neutron spectrum at the National Ignition Facility (NIF)“, Rev. Sci. Instrum. 87, 11D806 (2016).